Cerebrospinal fluid pressures during dynamic contusion-type spinal cord injury in a pig model

C.F. Jones[1,3], J.H.T. Lee[3], B. K. Kwon[2,3], P.A. Cripton[1,3]
[1] Orthopaedic and Injury Biomechanics Group, Departments of Mechanical Engineering and Orthopaedics, [2] Division of Spine, Department of Orthopaedics and
[3]International Collaboration on Repair Discoveries;
The University of British Columbia, Vancouver, Canada.

ABSTRACT

Despite considerable effort over the last four decades, research has failed to translate into tangible and consistently effective treatment options for spinal cord injury (SCI). This is partly attributed to differences between the human injury response and that of the predominant rodent models. We hypothesized that some of this divergence could be because humans have a discernable cerebrospinal fluid (CSF) layer surrounding their spinal cord, while rodents do not. Therefore, we sought to characterize the fluid impulse induced in the CSF by experimental SCIs of low and high human-like severity, and to compare this with previous studies in which fluid impulse has been associated with neural tissue injury. We used a new in vivo pig model (n=6 per injury group, mean age 124.5 days, 20.9 kg) incorporating four miniature pressure transducers that were implanted in pairs in the subarachnoid space, cranial and caudal to the injury at 30 mm and 100 mm. The median peak impact force was 20.8 and 62.1 N, and the impact velocity, 2.3 and 4.7 m/s, for the low and high injury severities, respectively. The peak pressures near the injury had median values of 522.5 and 868.8 mmHg (range 96.7-1430.0) and far from the injury, 7.6 and 36.3 mmHg (range 3.8-83.7), for the respective injury groups. Pressure impulse, wave speed and attenuation factor were also evaluated. The data indicates that the severity and extent of primary tissue damage close to the injury site may be affected by a fluid pressure wave in the human-like CSF-spinal cord system. However, the pressure wave was considerably damped at 100 mm from the injury, reaching close to normal physiologic pressures. This study provides evidence that future work seeking to elucidate the mechanical origins of primary tissue damage in SCI should consider utilizing an animal or computational model that incorporates CSF. Further, this pig model may provide a valuable addition to the preclinical experimental process due to its similarities to human scaling, including the existence of a human-like CSF fluid layer.

INTRODUCTION

Despite concentrated research efforts over the past three decades, spinal cord injury (SCI) continues to be a devastating and permanent condition. While a number of treatments that showed promise in preclinical studies have been tested in human clinical trials, none have had demonstrable efficacy (Kwon, 2010). This lack of effective translation of treatments from laboratory models to bedside has been attributed, in part, to important differences between the human injury and the rodent models commonly used to represent it. While the rat contusion model replicates some features of human SCI (Tator, 1995), there are substantive differences in neuroanatomy and behavioral outcome (Courtine, 2007). One clear disadvantage of the rat model is the large discrepancy in scale relative to human anatomy (Jeffery, 2006). Recognizing this, there is a strong sentiment within the SCI research community that establishing preclinical treatment efficacy in a suitable large animal model would be an advantageous step in the appropriate preclinical evaluation of treatments (Kwon, 2010). Biomechanically, this size discrepancy has implications for the selection of suitable injury parameters, and the subsequent mechanical and biological response of the system to the injury and to treatment agents. We propose that an overlooked consideration to this scaling issue is the lack of a cerebrospinal fluid (CSF) layer of the same relative dimension as humans.

Humans have a CSF layer surrounding the spinal cord that is on the order of 2-4 mm thick in the thoracic region (Gellad, 1983; Zaaroor, 2006). Previous *ex vivo* and *in vivo* studies have noted the potential for this fluid layer to be both mechanically protective (e.g. Hung, 1975; Jones, 2008; Persson, 2009) and potentially injurious (Bunegin, 1987; Czeiter, 2008; Hung, 1975) depending on the nature and magnitude of the mechanical loading. For the latter, it has been proposed that a pressure wave of sufficient magnitude travelling away from the mechanical impact may injure cells some distance from the impact (Czeiter, 2008; Hung, 1975). Axonal injury remote from the site of mechanical impact has been observed clinically (Cornish, 2000; Shannon, 1998) and *in vivo* and *in vitro* neural tissues are adversely affected by experimental fluid impulses (e.g. Saljo, 2008; Shepard, 1991; Stalhammar, 1987). Despite this potential "over-pressure" mechanism, animal, cadaver, and computational models that are used to study the mechanisms of injury and treatment commonly do not include a fluid layer, and only one study has measured CSF pressure during an experimental SCI (Hung, 1975).

The objective of this study was to characterize the CSF pressure waves associated with experimental SCIs of low and high human-like severity, and determine if these are sufficient to contribute to neural tissue injury some distance from the primary mechanical insult.

METHODS

The experimental protocol was approved by the University of British Columbia Animal Care Committee and complied with the guidelines and policies of the Canadian Council on Animal Care. Twelve female Yucatan miniature pigs (~20 kg, Sinclair Bio-resources, Windham, ME, USA) were group housed and acclimatized at our facility for at least one week before surgery. Anaesthesia was induced with Telazol (4-6 mg/kg IM), animals were intubated, and maintained on isoflurane (2-2.5% in O_2) with mechanical ventilation (10-12 breaths/min, tidal volume 10-12 mL/kg). Analgesics (Hydromorphone 0.15mg/kg IM and morphine 1mg/kg IM)

and antibiotics (Cefazolin, 20mg/kg IV) were administered before surgery and thereafter as needed, and every 4 hours, respectively. Hydration was maintained with lactated Ringer's solution (IV). Temperature was monitored via rectal probe and maintained at 38.5°C with a circulating-water pad. Catheters were placed in the left carotid artery and external jugular vein to monitor arterial and venous pressure. A urinary catheter was placed suprapubically. Ventilation and anesthetic level were adjusted to maintain normal heart rate and blood pressure.

Injury device and pressure transducers

The SCI was imparted with a custom modified drop-weight device, using a load cell instrumented 20 g weight released from a height of 25 cm (low severity, n=6) or 125 cm (high severity, n=6), replicating the bone fragment weight and velocity associated with burst fractures (Hall, 2006; Panjabi, 1995). Details provided in Appendix A (figures A1, A2). A high speed camera (PhantomV9.1, Vision Research, Wayne, NJ, USA) was used to track quadrant markers rigidly attached to the weight and guide rail (field of view ~50x275 mm, 5500 frames per second, resolution 240x1344). The position of the dorsal spinal dura and guide rail markers were obtained in the same field of view immediately before injury using a custom digitizing probe. The images were used to determine weight velocity and dorsal dura displacement during injury. CSF, arterial and venous pressures were measured with miniature fiber-optic pressure transducers: two high range (-75-3500 mmHg) placed at 30 mm from the injury site (cranial-, caudal-near), and two low range (-37.5-262.5 mmHg) at 100 mm (cranial-, caudal-far) (Fig. A3).

Protocol

The animal was anaesthetized and the spinal cord was exposed via a laminectomy from T7 to T14. The laminectomy was widened at T10-T11 to ensure that the weight's impactor tip did not strike the bony edges during impact. Pedicle screws were inserted and the articulating arm attached. The pressure sensors were then inserted intrathecally and the guide rail attached and aligned vertically. The position of the dorsal dural surface was recorded with the digitizing probe. The animal's ventilation was held to cease respiration motion and the solenoid was activated to impart the injury. The ventilation was resumed within three seconds after injury. All animals remained under anaesthetic for 14 hours post-injury: 100 g compression for 8 hours and then 6 hours without compression (as part of a separate protocol). Spinal cords were harvested for histological analysis (results not reported here).

Data acquisition, analysis and statistics

Pressure and load data were acquired with custom Labview (V8.6, National Instruments, Austin, TX, USA) programs at 50 kHz then post-filtered and processed with custom Matlab (2008b, The Mathworks, Matick, MA, USA) code with a two-way 4th-order Butterworth filter with 5 kHz low-pass cutoff frequency. High speed video was captured with Phantom (v9.0.640, Vision Research Inc., Wayne, NJ, USA) and distortion corrected with a camera calibration routine (Bouguet, 2004). Markers were tracked using TEMA (V3.2-024, Image Systems AB, Linköping, Sweden). For each test we determined injury parameters: peak impact force, impulse, dorsal dural displacement, impact velocity; and pressure parameters: peak pressure, impulse, wave speed and attenuation ratio (Figure 1). All CSF pressures are reported relative to the pre-injury value to eliminate the effect of hydrostatic pressure variation (Carlson, 2003) and respiratory and vascular pulsations. We assessed the model (animal age, weight, pre-injury CSF pressure), injury and pressure parameters using non-parametric descriptive statistics. Differences

between these parameters for the two experimental groups were assessed with Mann-Whitney U Tests. Wilcoxon Rank Sum matched-pairs tests were used to assess differences in the pressure profiles caudal and cranial to the injury. Significance level was 0.05 for all tests.

RESULTS

Each animal group was consistent in age and weight and the model produced two distinct and repeatable injury parameter groups. The high severity injuries had a mean peak impact force three times higher than, and mean load impulse and impact velocities twice as high as, the low severity injuries; these differences were statistically significant. The mean dural displacement was similar for the two groups. The pre-injury CSF pressure was within the normal range; however, there was a trend towards lower initial pressures for the low severity group (Table 1).

Table 1: Descriptive statistics for model assessment parameters and results of Mann-Whitney U-tests comparing these parameters for the low and high severity injury groups

	Age (days)	**Weight (kg)**	**Pre-injury CSF pressure Cr/Ca (mmHg)**	**Peak impact force (N)**	**Load impulse (N.ms)**	**Impact velocity (m/s)**	**Dural dsplmt. (mm)**
Low	121.5 *(115.0,133.0)*	20.0 *(20.0, 20.0)*	5.0/4.4 *(4.4,6.7)/(3.0,6.3)*	20.8* *(18.4, 21.1)*	53.9* *(53.0, 57.9)*	2.3** *(2.3, 2.3)*	9.2*** *(7.1, 11.2)*
High	124.0 *(121.0,130.0)*	21.3 *(19.5, 24.0)*	7.8/7.6 *(6.0,8.2)/(6.7,8.7)*	62.1 *(53.0, 65.1)*	101.5 *(98.3,101.7)*	4.7* *(4.5, 4.8)*	8.3* *(7.5, 10.2)*
p	0.589	0.485	0.132/0.041	0.004	0.004	0.036	1.000

Cr=cranial, Ca=caudal ; n=6 except: *n=5 **n=3 ***n=2

In all animals distinct pressure pulses of magnitudes greater than normal physiologic values were observed at the four transducer locations. The pulse at the "near" transducers had greater peak magnitude, greater impulse and shorter duration than the "far" transducers, both caudal and cranial, and for both injury severities. A typical response is shown in Figure 1, below.

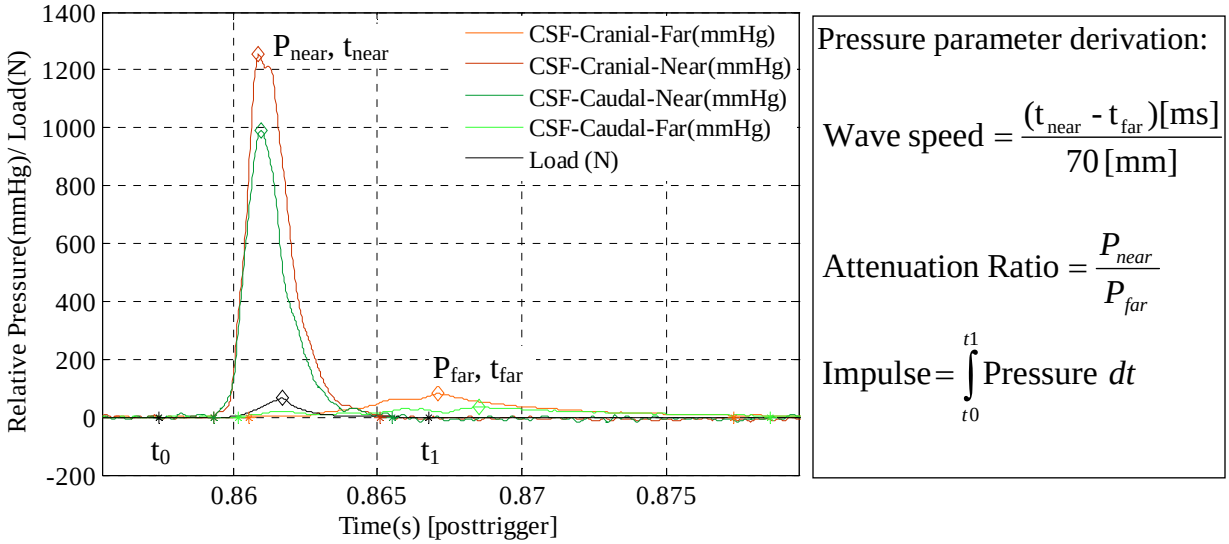

Figure 1: Typical response for a single injury (#P1805); CSF pressure at four locations, and load. Open diamonds indicate peak pressure, *indicate impulse calculation bounds. (right) Parameter equations.

The high severity injury was associated with greater peak pressures and impulses; however, due to considerable variation in specimen response this was not statistically significant for all transducer locations (Figure 2). The estimated wave speeds had an overall range of 2.5-15.5 m/s and a non-significant trend towards higher speeds for the high severity injury. The attenuation ratio between the near and far locations ranged from 9.3 to 106.6 and there was no significant difference in its magnitude between the injury groups.

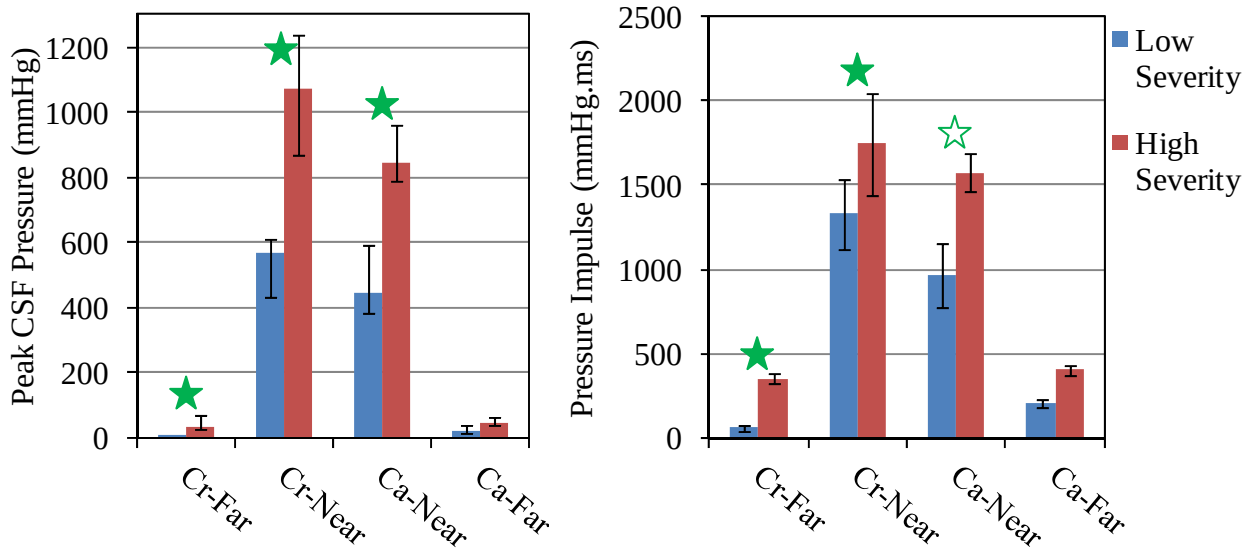

Figure 2: Peak CSF pressure and pressure impulse at each transducer location, for two injury groups. Bar is median value, error bars are 25th%ile/75th%ile. ★significance; ☆marginal significance.

There was no significant association between the cranial/caudal location and the magnitude of the pressure peak or impulse at either the "near" or "far" transducers. Wave speed was significantly greater on the caudal than the cranial side (mean 1.2-1.8 times), while attenuation factor tended to be greater for the cranial side, but did not reach significance. Appendix B presents some additional details of the results.

DISCUSSION

We have demonstrated the utility and repeatability of a novel large animal model of thoracic contusive SCI, and have measured the cranial and caudal CSF pressure variation associated with two simulated bony impingement velocities approximating low and high severity human SCI. We characterized the CSF pressure wave with the parameters of peak pressure, pressure impulse, attenuation ratio and wave speed.

Dynamic CSF and neural parenchyma pressures have been measured intracranially in various models of traumatic brain injury (TBI) (Clausen, 2005; Krave, 2005; Nahum, 1977; Saljo, 2008; Stalhammar, 1987; Suneson, 1990), and in the spine during simulated whiplash (e.g. Boström, 1996; Eichberger, 2000). To the authors' knowledge, pressures relating to acute SCI have been investigated only in synthetic/cadaver models (Pintar, 1995; Yoganandan, 1995) and in a single cat during *in vivo* experimental SCI (Hung, 1975). In general, the form of the pressure profiles measured here was similar to those reported for impact of the brain and spinal cord. A notable difference was the absence of an appreciable negative pressure trough preceding the

positive pressure peak. We observed this in previous tests using this model when 1) only one transducer was implanted at each far location, 2) more severe injuries were applied and, 3) a spherical impactor tip was used (Jones, 2009). It is not apparent what caused this difference.

The peak pressures measured at the "near" locations were in excess of normal values that have been recorded in recumbent large animals, 8.8-10 mmHg (Carlson, 2003; Klarica, 2006) and humans, 6.6-20.6 mmHg (Eidlitz-Markus, 2005; Greenfield, 1984; Whiteley, 2006). Comparing our closest condition of the "near" transducers with the low severity injury, our peak pressure range of 96.7-680.2 mmHg, is considerably higher than the 50 mmHg peak of Hung (1975). This may be due to differences in animal size, injury parameters (15g-25cm for Hung vs. 20g-32cm) and pressure transducer configuration. That study used a pressure transducer that was fluid-coupled via a catheter and tubing which can cause damping of the signal, whereas our transducers were indwelling and the sensing face was directed toward the injury site.

The reduction in peak pressure and impulse from the "near" to "far" locations was expected and is due to dampening of the wave via energy absorption by the cord and dural tissues. Also the "far" transducers did not face the direction of the impulse-induced flow due to restrictions of anatomical size. In general, the pressure peaks measured at the "far" location (range 1.7-93.0 mmHg, relative to pre-injury baseline) were of a similar order of magnitude to increases measured in man during transient increased intra-abdominal pressure (10.5 mmHg valsalva maneuver (Greenfield, 1984)), jugular occlusion (10.7 mmHg, Queckenstedt's test), and coughing (~50 mmHg) (Williams, 1981). These have no physiologic effect when performed transiently and normal autoregulation mechanisms are functioning. Therefore, it would be reasonable to conclude that pressure-induced injury is unlikely at the "far" location. The 10 to 100-fold attenuation ratios also indicate that for the injury severities used in this study, sufficient energy is absorbed from the fluid into the cord and dura by at least 100 mm from the injury site.

We had expected that the wave speed would be greater for the higher injury severity but this parameter exhibited large variation, and its magnitude appeared independent of injury parameters. The differences in caudal and cranial response, although limited to wave speed and marginally attenuation ratio, may indicate that the end condition (cranially the ventricles and brain, and caudally the lumbar cistern) has a limited effect on the fluid wave propagation.

To the authors' knowledge, there is no established pressure tolerance value for the bulk spinal cord or its cellular constituents. However, recent studies investigating diffuse axonal brain injury due to blast overpressure exposure have indicated that pressure-related injury thresholds may be lower for neural tissue than other soft tissue and organs (Kato, 2007). Animals exposed to external overpressures ranging from 75 to 7500 mmHg have exhibited reduced performance in physical tests and degeneration of cerebral cortex neurons (Moochhala, 2004), injury to neuronal and glial cells, and brain edema (Kaur, 1995; Saljo, 2000; Saljo, 2001; Saljo, 2002a; Saljo, 2002b; Svetlov, 2010), brain haemorrhage and edema (Saljo, 2008), morphological changes to neurons (Kato, 2007), damage to central visual pathways (Petras, 1997) and elevated intracranial pressure and impaired cognitive function (Saljo, 2009).

In vitro cell preparations have also been subjected to pressure impulses to induce injury, with magnitudes similar to those recorded in our study. Neuronal and glial cells exposed to fluid

pressure impulses of 1550 mmHg (Suneson, 1989) and 362-3050 mmHg (Shepard, 1991) show cell damage and reduced viability. These preparations typically restrict the ability of the tissue to undergo concomitant strain deformation (Morrison, 1998), which provides support for the mechanism of pressure induced injury in the absence of other mechanical loading. Dynamic intracranial pressures of 1800-4000 mmHg have been recorded during fluid-percussion TBI (e.g. Clausen, 2005; Stalhammar, 1987; Walter, 1999). These pressures were associated with severe brain injury and encompass the higher range measured in our study.

The pressure impulse for the various models discussed above is not commonly reported. However, it has been noted that pressure impulse may be a superior injury determinant than peak pressure for some cells (Kodama, 2000), and load impulse is commonly used in injury biomechanics as tissue tolerance is often better expressed by both the magnitude of a load and the duration of its application. For the fluid percussion model in cats, Hayes (1987) reported irreversible apnea with a fluid impulse in the brain of 7600 mmHg.ms, while Saljo (2008) measured impulses ranging 37-590 mmHg.ms and reported cellular damage in the brain of pigs subjected to low impulse noise from firearms. The impulses recorded at the “near” location in our study are between these two ranges, and at the “far” location are generally within the range of Saljo (2008); however, the lack of data makes it difficult to draw conclusions about the likelihood of cellular injury.

This injury model faces challenges common to all large animal studies; most notably time, cost and complexity. However, it offers many advantages over the conventional rat SCI models, the most pertinent being the approximate human scale, the associated presence of CSF, and the similarities to human anatomy and physiology. Other limitations include the necessary alteration of the biomechanical system by laminectomy, removal of ligamentum flavum and dorsal epidural fat, and insertion of transducers. The laminectomy width and length was minimized, and by using small and flexible transducers we minimized their effect on mechanical response. While the transducer faces were not shielded, the fibers ran parallel to the cord in the intrathecal space and the sensing face is on the cross-section of the fiber. There was a learning curve associated with transducer insertion which probably led to the differing pre-injury CSF pressure between the two groups; however, this is unlikely to have altered the observed trends due to the large difference in the injury parameters for the two groups.

This study presents the first characterization of CSF pressure impulses associated with SCI. The significant strengths of this study are that the model has human-like dimensions and physiology, we used injury parameters that approximate the human injury event to the best available knowledge, we used multiple miniature indwelling pressure transducers that minimized changes to the biomechanics of the system and we described the resultant fluid impulses with several quantitative parameters. When compared to previous studies linking pressure impulses and cellular damage in the brain, the data indicates that the severity of primary tissue damage may be affected by the propagating fluid pressure wave, and that the cranial-caudal extent of this injury may be limited by the damping effect of the neural and dural tissue, which in this study reduced the pressure close to normal ranges within 100 mm of the injury site. The data suggest that the design and implementation of future animal, cadaver and computational models that seek to accurately replicate the biomechanics of human SCI should consider the inclusion of CSF, and this data will be valuable for the validation of such models.

ACKNOWLEDGEMENTS

The invaluable support and technical assistance of Gordon Gray, Tamera Godbey, Bev Chua, Rhonda Hildebrandt, Kari Jones, Uri Burstyn, Anthea Stammers, Elena Okon, Marcus Fengler, Glenn Jolly and Robyn Newell is gratefully acknowledged. This project is supported by funding from the Canadian Institute of Health Research (PAC/BKK) and the Natural Sciences and Engineering Research Council (Canada) (PAC).

REFERENCES

BOSTRÖM, O., SVENSSON, M.Y., ALDMAN, B., HANSSON, H.A., HAALAND, Y., LÖVSUND, P., SEEMAN, T., SUNESON, A., SÄLJÖ, A. and ÖRTENGREN, T. (1996). A New Neck Injury Criterion Candidate-Based on Injury Findings in the Cervical Spinal Ganglia after Experimental Neck Extension Trauma. International IRCOBI conference on the Biomechanics of Impact: Dublin, Sept. 11-13.

BOUGUET, J.-Y. (2004). Camera Calibration Toolbox for Matlab: California Institute of Technology, Pasadena, CA, USA. Available at: [http://www.vision.caltech.edu/bouguetj/index.html], Last updated June 2008.

BUNEGIN, L., HUNG, T.K. and CHANG, G.L. (1987). Biomechanics of Spinal Cord Injury. Crit Care Clin. **3**:453-470.

CARLSON, G.D., OLIFF, H.S., GORDEN, C., SMITH, J. and ANDERSON, P.A. (2003). Cerebral Spinal Fluid Pressure: Effects of Body Position and Lumbar Subarachnoid Drainage in a Canine Model. Spine. **28**:119-122.

CLAUSEN, F. and HILLERED, L. (2005). Intracranial Pressure Changes During Fluid Percussion, Controlled Cortical Impact and Weight Drop Injury in Rats. Acta Neurochir (Wien). **147**:775-780; discussion 780.

CORNISH, R., BLUMBERGS, P.C., MANAVIS, J., SCOTT, G., JONES, N.R. and REILLY, P.L. (2000). Topography and Severity of Axonal Injury in Human Spinal Cord Trauma Using Amyloid Precursor Protein as a Marker of Axonal Injury. Spine (Phila Pa 1976). **25**:1227-1233.

COURTINE, G., BUNGE, M.B., FAWCETT, J.W., GROSSMAN, R.G., KAAS, J.H., LEMON, R., MAIER, I., MARTIN, J., NUDO, R.J., RAMON-CUETO, A., ROUILLER, E.M., SCHNELL, L., WANNIER, T., SCHWAB, M.E. and EDGERTON, V.R. (2007). Can Experiments in Nonhuman Primates Expedite the Translation of Treatments for Spinal Cord Injury in Humans? Nat Med. **13**:561-566.

CZEITER, E., PAL, J., KOVESDI, E., BUKOVICS, P., LUCKL, J., DOCZI, T. and BUKI, A. (2008). Traumatic Axonal Injury in the Spinal Cord Evoked by Traumatic Brain Injury. J Neurotrauma. **25**:205-213.

DALGREN, M. (2010). Personal Communication. Frequency Response of Samba Pressure Transducers.

EICHBERGER, A., DAROK, M., STEFFAN, H., LEINZINGER, P.E., BOSTROM, O. and SVENSSON, M.Y. (2000). Pressure Measurements in the Spinal Canal of Post-Mortem Human Subjects During Rear-End Impact and Correlation of Results to the Neck Injury Criterion. Accid Anal Prev. **32**:251-260.

EIDLITZ-MARKUS, T., STIEBEL-KALISH, H., RUBIN, Y. and SHUPER, A. (2005). CSF Pressure Measurement During Anesthesia: An Unreliable Technique. Paediatr Anaesth. **15**:1078-1082.

GELLAD, F., RAO, K.C., JOSEPH, P.M. and VIGORITO, R.D. (1983). Morphology and Dimensions of the Thoracic Cord by Computer-Assisted Metrizamide Myelography. AJNR Am J Neuroradiol. **4**:614-617.

GREENFIELD, J.C., JR., REMBERT, J.C. and TINDALL, G.T. (1984). Transient Changes in Cerebral Vascular Resistance During the Valsalva Maneuver in Man. Stroke. **15**:76-79.

HALL, R.M., OAKLAND, R.J., WILCOX, R.K. and BARTON, D.C. (2006). Spinal Cord-Fragment Interactions Following Burst Fracture: An in Vitro Model. J Neurosurg Spine. **5**:243-250.

HAYES, R.L., STALHAMMAR, D., POVLISHOCK, J.T., ALLEN, A.M., GALINAT, B.J., BECKER, D.P. and STONNINGTON, H.H. (1987). A New Model of Concussive Brain Injury in the Cat Produced by Extradural Fluid Volume Loading: Ii. Physiological and Neuropathological Observations. Brain Inj. **1**:93-112.

HUNG, T.K., ALBIN, M.S., BROWN, T.D., BUNEGIN, L., ALBIN, R. and JANNETTA, P.J. (1975). Biomechanical Responses to Open Experimental Spinal Cord Injury. Surg Neurol. **4**:271-276.

JEFFERY, N.D., SMITH, P.M., LAKATOS, A., IBANEZ, C., ITO, D. and FRANKLIN, R.J. (2006). Clinical Canine Spinal Cord Injury Provides an Opportunity to Examine the Issues in Translating Laboratory Techniques into Practical Therapy. Spinal Cord. **44**:584-593.

JONES, C.F., KROEKER, S.G., CRIPTON, P.A. and HALL, R.M. (2008). The Effect of Cerebrospinal Fluid on the Biomechanics of Spinal Cord: An Ex Vivo Bovine Model Using Bovine and Physical Surrogate Spinal Cord. Spine (Phila Pa 1976). **33**:E580-588.

JONES, C.F., KWON, B.K. and CRIPTON, P.A. (2009). Cerebrospinal Fluid Pressures Measured During Spinal Cord Injury in a Novel Pig Model [Abstract]. In: *Neurotrauma 2009: Second Joint Symposium of the International and National Neurotrauma Societies, September 7-11*. Journal of Neurotrauma.: Santa Barbara, California, pps. A-49.

KATO, K., FUJIMURA, M., NAKAGAWA, A., SAITO, A., OHKI, T., TAKAYAMA, K. and TOMINAGA, T. (2007). Pressure-Dependent Effect of Shock Waves on Rat Brain:

Induction of Neuronal Apoptosis Mediated by a Caspase-Dependent Pathway. J Neurosurg. **106**:667-676.

KAUR, C., SINGH, J., LIM, M.K., NG, B.L., YAP, E.P. and LING, E.A. (1995). The Response of Neurons and Microglia to Blast Injury in the Rat Brain. Neuropathol Appl Neurobiol. **21**:369-377.

KLARICA, M., RADOS, M., DRAGANIC, P., ERCEG, G., ORESKOVIC, D., MARAKOVIC, J. and BULAT, M. (2006). Effect of Head Position on Cerebrospinal Fluid Pressure in Cats: Comparison with Artificial Model. Croat Med J. **47**:233-238.

KODAMA, T., HAMBLIN, M.R. and DOUKAS, A.G. (2000). Cytoplasmic Molecular Delivery with Shock Waves: Importance of Impulse. Biophys J. **79**:1821-1832.

KRAVE, U., HOJER, S. and HANSSON, H.A. (2005). Transient, Powerful Pressures Are Generated in the Brain by a Rotational Acceleration Impulse to the Head. Eur J Neurosci. **21**:2876-2882.

KWON, B.K., HILLYER, J. and TETZLAFF, W. (2009). Translational Research in Spinal Cord Injury: A Survey of Opinion from the SCI Community. J Neurotrauma. **27**(1): 21-33.

MOOCHHALA, S.M., MD, S., LU, J., TENG, C.H. and GREENGRASS, C. (2004). Neuroprotective Role of Aminoguanidine in Behavioral Changes after Blast Injury. J Trauma. **56**:393-403.

MORRISON, B., 3RD, SAATMAN, K.E., MEANEY, D.F. and MCINTOSH, T.K. (1998). In Vitro Central Nervous System Models of Mechanically Induced Trauma: A Review. J Neurotrauma. **15**:911-928.

NAHUM, A.M., SMITH, R. and WARD, C.C. (1977). Intracranial Pressure Dynamics During Head Impact. In: *21st Stapp Car Crash Conference*. SAE (ed). SAE International, Warrendale, Pennsylvania, USA: New Orleans, Louisiana, USA, pps. 339-366.

PANJABI, M.M., KIFUNE, M., WEN, L., ARAND, M., OXLAND, T.R., LIN, R.M., YOON, W.S. and VASAVADA, A. (1995). Dynamic Canal Encroachment During Thoracolumbar Burst Fractures. J Spinal Disord. **8**:39-48.

PERSSON, C., MCLURE, S.W., SUMMERS, J. and HALL, R.M. (2009). The Effect of Bone Fragment Size and Cerebrospinal Fluid on Spinal Cord Deformation During Trauma: An Ex Vivo Study. J Neurosurg Spine. **10**:315-323.

PETRAS, J.M., BAUMAN, R.A. and ELSAYED, N.M. (1997). Visual System Degeneration Induced by Blast Overpressure. Toxicology. **121**:41-49.

PINTAR, F.A., YOGANANDAN, N., MAIMAN, D.J. and SANCES, A.J. (1995). Cervical Spinal Bony Injury and the Potential for Cord Injury. In: *5th Symposium on Injury Prevention Through Biomechanics*. GRIMM, M.J. (ed): Detroit, pps. 161-169.

SALJO, A., BAO, F., HAGLID, K.G. and HANSSON, H.A. (2000). Blast Exposure Causes Redistribution of Phosphorylated Neurofilament Subunits in Neurons of the Adult Rat Brain. J Neurotrauma. **17**:719-726.

SALJO, A., BAO, F., HAMBERGER, A., HAGLID, K.G. and HANSSON, H.A. (2001). Exposure to Short-Lasting Impulse Noise Causes Microglial and Astroglial Cell Activation in the Adult Rat Brain. Pathophysiology. **8**:105-111.

SALJO, A., BAO, F., JINGSHAN, S., HAMBERGER, A., HANSSON, H.A. and HAGLID, K.G. (2002a). Exposure to Short-Lasting Impulse Noise Causes Neuronal C-Jun Expression and Induction of Apoptosis in the Adult Rat Brain. J Neurotrauma. **19**:985-991.

SALJO, A., BAO, F., SHI, J., HAMBERGER, A., HANSSON, H.A. and HAGLID, K.G. (2002b). Expression of C-Fos and C-Myc and Deposition of Beta-App in Neurons in the Adult Rat Brain as a Result of Exposure to Short-Lasting Impulse Noise. J Neurotrauma. **19**:379-385.

SALJO, A., ARRHEN, F., BOLOURI, H., MAYORGA, M. and HAMBERGER, A. (2008). Neuropathology and Pressure in the Pig Brain Resulting from Low-Impulse Noise Exposure. J Neurotrauma. **25**:1397-1406.

SALJO, A., SVENSSON, B., MAYORGA, M., HAMBERGER, A. and BOLOURI, H. (2009). Low Levels of Blast Raises Intracranial Pressure and Impairs Cognitive Function in Rats. J Neurotrauma. **26**(8)1345-1352.

SHANNON, P., SMITH, C.R., DECK, J., ANG, L.C., HO, M. and BECKER, L. (1998). Axonal Injury and the Neuropathology of Shaken Baby Syndrome. Acta Neuropathol. **95**:625-631.

SHEPARD, S.R., GHAJAR, J.B., GIANNUZZI, R., KUPFERMAN, S. and HARIRI, R.J. (1991). Fluid Percussion Barotrauma Chamber: A New in Vitro Model for Traumatic Brain Injury. J Surg Res. **51**:417-424.

STALHAMMAR, D., GALINAT, B.J., ALLEN, A.M., BECKER, D.P., STONNINGTON, H.H. and HAYES, R.L. (1987). A New Model of Concussive Brain Injury in the Cat Produced by Extradural Fluid Volume Loading: I. Biomechanical Properties. Brain Inj. **1**:73-91.

SUNESON, A., HANSSON, H.A., LYCKE, E. and SEEMAN, T. (1989). Pressure Wave Injuries to Rat Dorsal Root Ganglion Cells in Culture Caused by High-Energy Missiles. J Trauma. **29**:10-18.

SUNESON, A., HANSSON, H.A. and SEEMAN, T. (1990). Pressure Wave Injuries to the Nervous System Caused by High-Energy Missile Extremity Impact: Part Ii. Distant Effects on the Central Nervous System--a Light and Electron Microscopic Study on Pigs. J Trauma. **30**:295-306.

SVETLOV, S.I., PRIMA, V., KIRK, D.R., GUTIERREZ, H., CURLEY, K.C., HAYES, R.L. and WANG, K.K. (2010). Morphologic and Biochemical Characterization of Brain Injury in a Model of Controlled Blast Overpressure Exposure. J Trauma. 2010 Mar 2. [Epub ahead of print]

TATOR, C.H. (1995). Update on the Pathophysiology and Pathology of Acute Spinal Cord Injury. Brain Pathol. **5**:407-413.

WALTER, B., BAUER, R., FRITZ, H., JOCHUM, T., WUNDER, L. and ZWIENER, U. (1999). Evaluation of Micro Tip Pressure Transducers for the Measurement of Intracerebral Pressure Transients Induced by Fluid Percussion. Exp Toxicol Pathol. **51**:124-129.

WHITELEY, W., AL-SHAHI, R., WARLOW, C.P., ZEIDLER, M. and LUECK, C.J. (2006). Csf Opening Pressure: Reference Interval and the Effect of Body Mass Index. Neurology. **67**:1690-1691.

WILLIAMS, B. (1981). Simultaneous Cerebral and Spinal Fluid Pressure Recordings. I. Technique, Physiology, and Normal Results. Acta Neurochir (Wien). **58**:167-185.

YOGANANDAN, N., PINTAR, F.A., MAIMAN, D.J., CUSICK, J.F. and SANCES JR., A. (1995). Cervical Spinal Cord Injury Using Biomechanical Experimentation. In: *39th Annual Proceedings of the Association for the Advancement of Automotive Medicine*. Association for the Advancement of Automotive Medicine, Des Plaines, Illinois, USA: Chicago, Illinois, USA.

ZAAROOR, M., KOSA, G., PERI-ERAN, A., MAHARIL, I., SHOHAM, M. and GOLDSHER, D. (2006). Morphological Study of the Spinal Canal Content for Subarachnoid Endoscopy. Minimially Invasive Neurosurgery. **49**:220-226.

AUTHOR LIST

1. Claire F. Jones
   Orthopaedic and Injury Biomechanics Lab
   Blusson Spinal Cord Centre
   818 W 10th Ave,
   Vancouver, BC
   V5Z 1M9
   Canada.
   Ph: 604 675 8845
   cfjones@mech.ubc.ca

2. Jae H.T. Lee
   Kwon Lab
   Blusson Spinal Cord Centre
   818 W 10th Ave,
   Vancouver, BC
   V5Z 1M9
   Canada.
   Ph: 604 675 8837
   jaelee@icord.ca

3. Brian K .Kwon
   Kwon Lab
   Blusson Spinal Cord Centre
   818 W 10th Ave,
   Vancouver, BC
   V5Z 1M9
   Canada.
   Ph: 604 875 5857
   Brian.Kwon@vch.ca

4. Peter A. Cripton
   Orthopaedic and Injury Biomechanics Lab
   Blusson Spinal Cord Centre
   818 W 10th Ave,
   Vancouver, BC
   V5Z 1M9
   Canada.
   Ph: 604 675 8835
   cripton@mech.ubc.ca

APPENDIX A: SUPPLEMENTARY METHODS

Injury Device

The injury device was attached to the spine unilaterally at T10-T13 with pedicle screws and a bridging titanium rod (screws: 4.0x26/28 mm; rod: 3.5 mm diameter/150 mm length; Vertex Reconstruction System, Medtronic, Minneapolis, MN, USA). This construct fixed to the base of an articulating arm (Model 660 (modified), L.S. Starett, Athol, MA, USA) which enabled the aluminum guide rail (N17, Igus, Concord, ON, Canada) to be placed orthogonal to the spinal cord, resting against the dorsal canal. The weight consisted of a rapid-prototyped hollow cylinder (material: ABS-M30, sealed with acrylic lacquer) with a linear bearing attachment (aluminum/plastic, Drylin N17, Igus, Concord, ON, Canada) and was instrumented with a load cell (subminiature load cell, 222.41 N, LLB215 (modified), Futek Advanced Sensor Technology, Irvine, CA, USA) to which a 3/8" diameter cylindrical impact tip (material: ABS-M30, sealed with acrylic lacquer) with 45°/1 mm beveled edge was fixed. This diameter closely matched the lateral diameter of the thoracic dura, as measured by *in vivo* magnetic resonance imaging (unpublished). The impact tip height was set using a custom measuring tool and the weight was released by a latching solenoid (STA151082-234-1002, cage 81840, Saia-Burgess, Vandalia, OH, USA) with associated custom electronics. (Figure A-1. A-2)

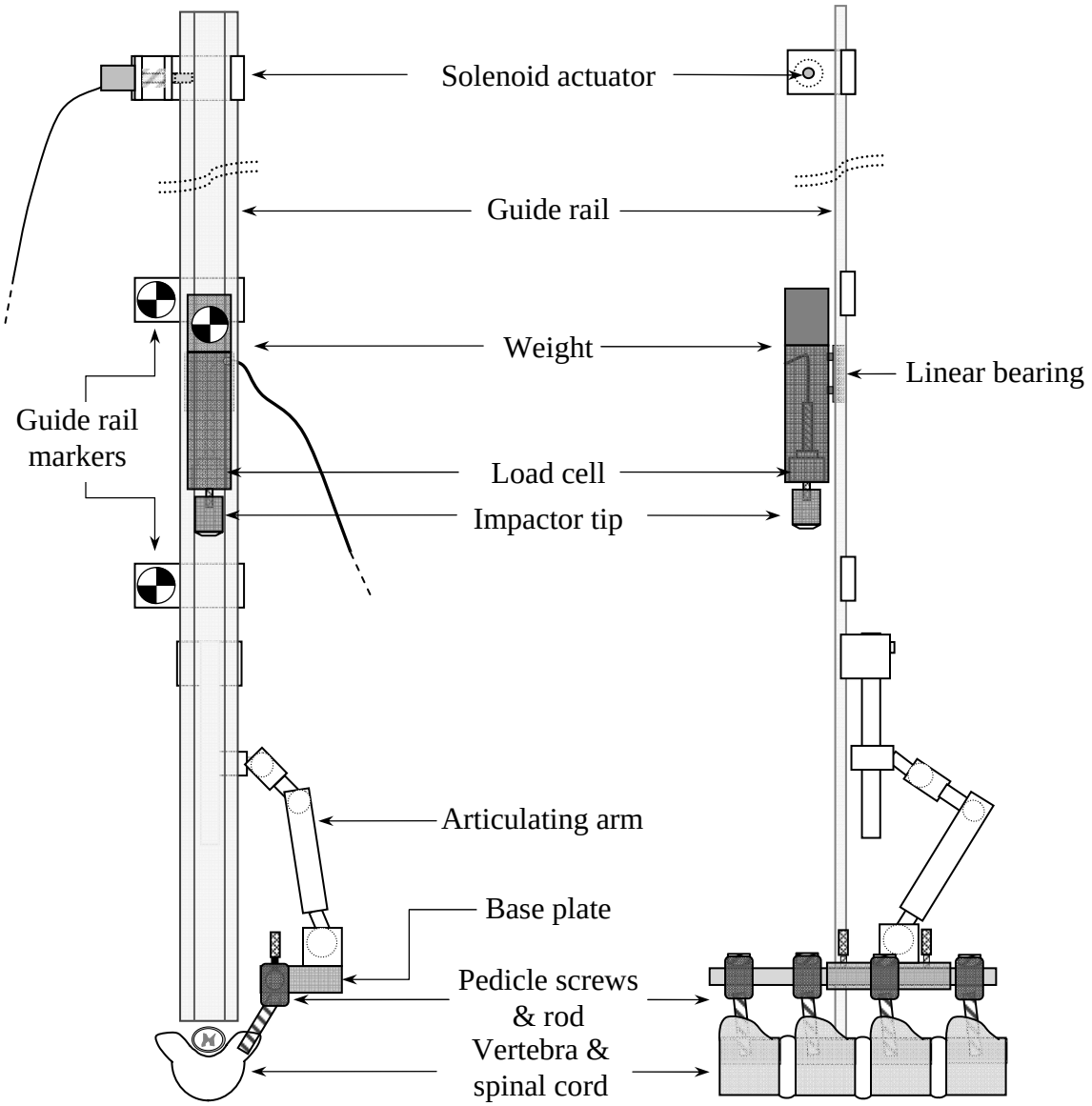

Figure A-1: Schematic of front view (left) and side view (right) of the drop-weight device installed on vertebra T10-T13.

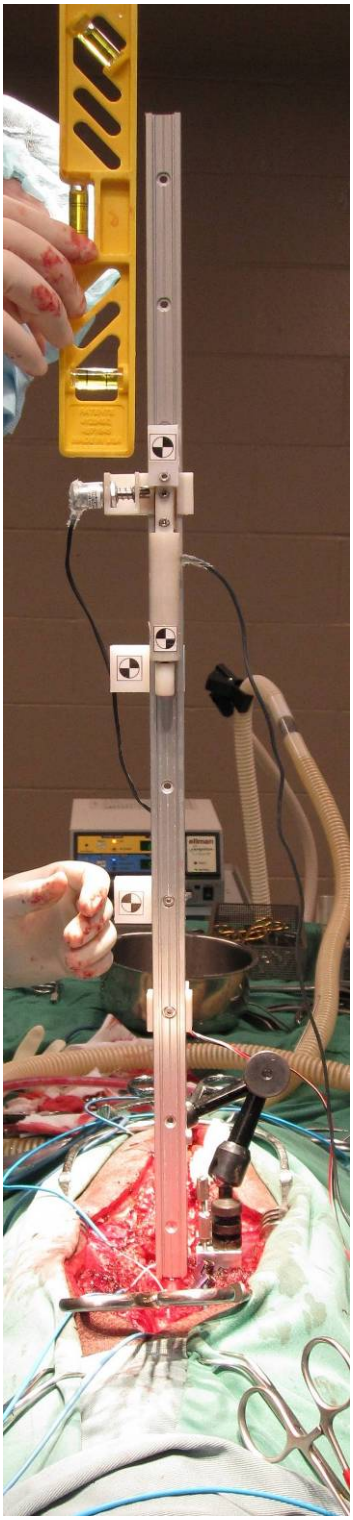

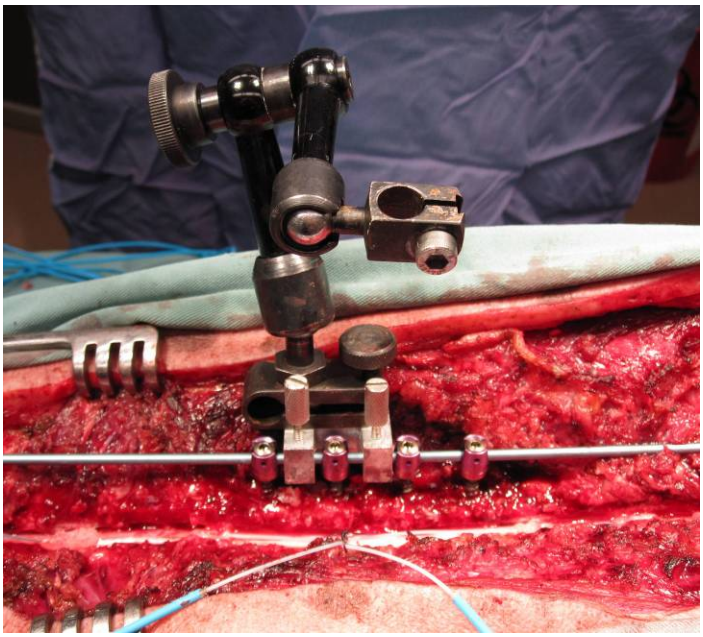

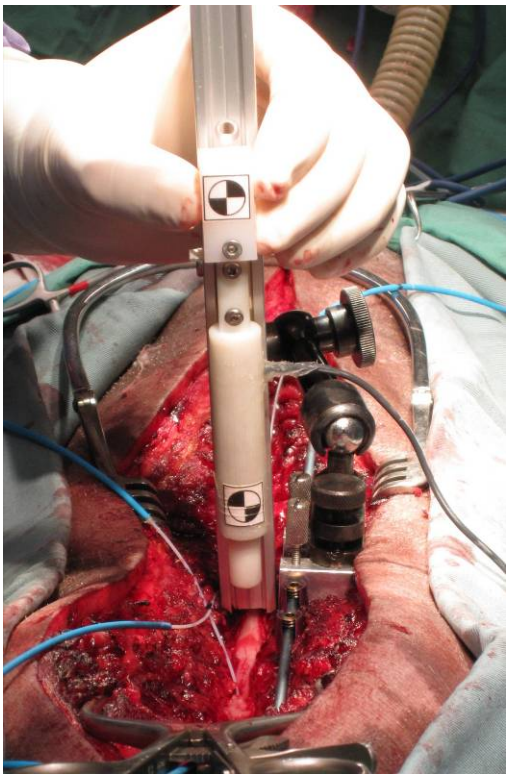

Figure A-2: Photos of experimental setup. Left: Drop weight apparatus installed and being aligned; Right, top: detail of device attachment to vertebra via pedicle screws; Right, bottom: checking alignment of the weight prior to a test, showing position of guide rail and impactor tip with respect to the spinal cord.

Pressure Transducers

Arterial and venous pressure transducers

Central arterial and venous catheters were placed surgically in the left carotid artery and external jugular vein. This catheter configuration allowed for introduction of, and sealing around, the fibre-optic transducer while maintaining a parallel access port for sampling and flushing. We used a 16 Ga, 15cm length catheter (Arrow/Teleflex Medical, Markam, Ontario, Canada) fitted with a Y-connector. One side of the Y was fitted with a Tuohy Borst adapter (84044/80369, Quosina, NY, USA) to seal over pressure transducer shaft, and the other side with a standard IV needle access port. The line was locked with heparin saline and flushed periodically to maintain patency.

Intrathecal pressure transducers

Intrathecal pressure transducers were placed after exposure of the dura. The surgical table was tilted so that the animal's head was angled downwards. The location of entry was measured with calipers and marked. The dorsal dura was gently lifted with forceps at this location and a small hole made with a needle tip. The transducer was rapidly introduced and advanced 50 mm into the intrathecal space, on the dorsal aspect of the cord. The dural hole was sealed around a small bone wax plug on the fiber, with cyanoacrylate adhesive gel. After all four transducers had been placed, the animal's head was raised to bring the thoracic spinal cord into a horizontal position.

Pressure transducer specifications

We used miniature fiber-optic pressure transducers (Table A-1) in combination with Samba Control Unit 202s. These control units sampled at a frequency at 40 kHz and the analog output was connected to National Instruments data acquisition hardware.

Table A-1: Pressure transducer specifications (Samba Sensors, Gruvgatan 6, Sweden)

Preclin420LP (low range)	Preclin360HP (high range)
Range: -37.5 - 262.5 mmHg Accuracy: ±0.38 mmHg plus ±2.5% of reading Sensor tip diameter: 0.42 mm Fiber diameter: 0.25 mm Temp. coeff.: <0.15 mmHg/ºC (20-45ºC/ 68-113ºF) w/o radiopaque coating	Range: -75 - 3500 mmHg Accuracy: ± 4% of reading Sensor tip diameter: 0.36 mm Fiber diameter: 0.40 mm Temp. coeff.: <2.6 mbar/ºC (20-45ºC/ 68-113ºF) w/ radiopaque coating
Bare fiber length: 50 mm Long term stability: <0.5% range. Frequency response: "There is no bandwidth limitation in the transducer or the control unit to affect the output rate of 40 kHz. The system can detect and indicate a full range pressure shift from one sample to the next. There is no "history-effect" or dampening/filtering. The limitation of the transducer is estimated to be about 1 MHz based on FEM simulations and material analysis." (Dalgren, 2010)	

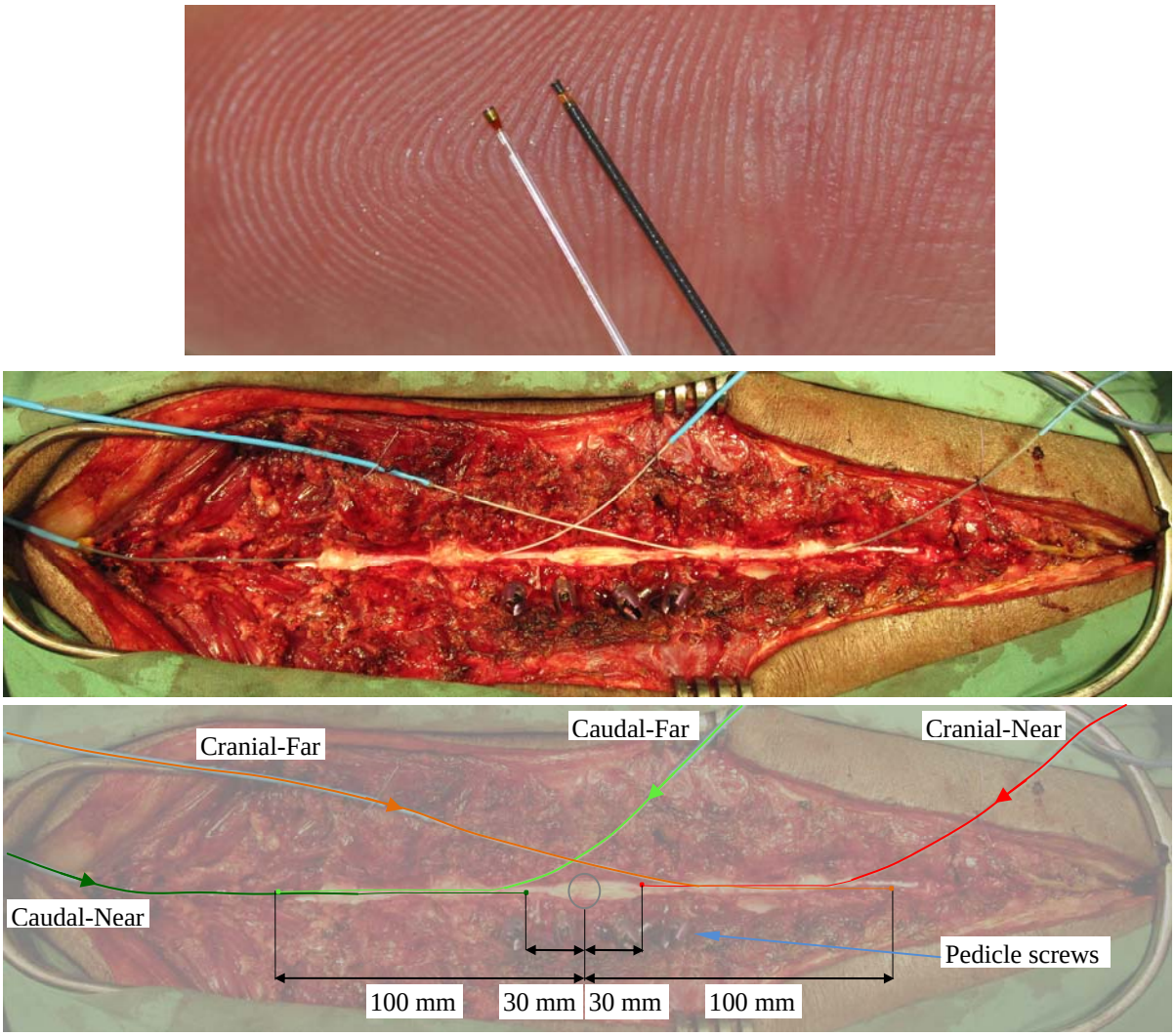

Figure A-3: Top: Photo of the low range (Preclin460LP) and high range (Preclin360HP, with radiopaque coating) pressure transducers, relative to the human finger print. Bottom: Photo and overlay indicating the location of the four intrathecal pressure transducers.

Parameter Derivation

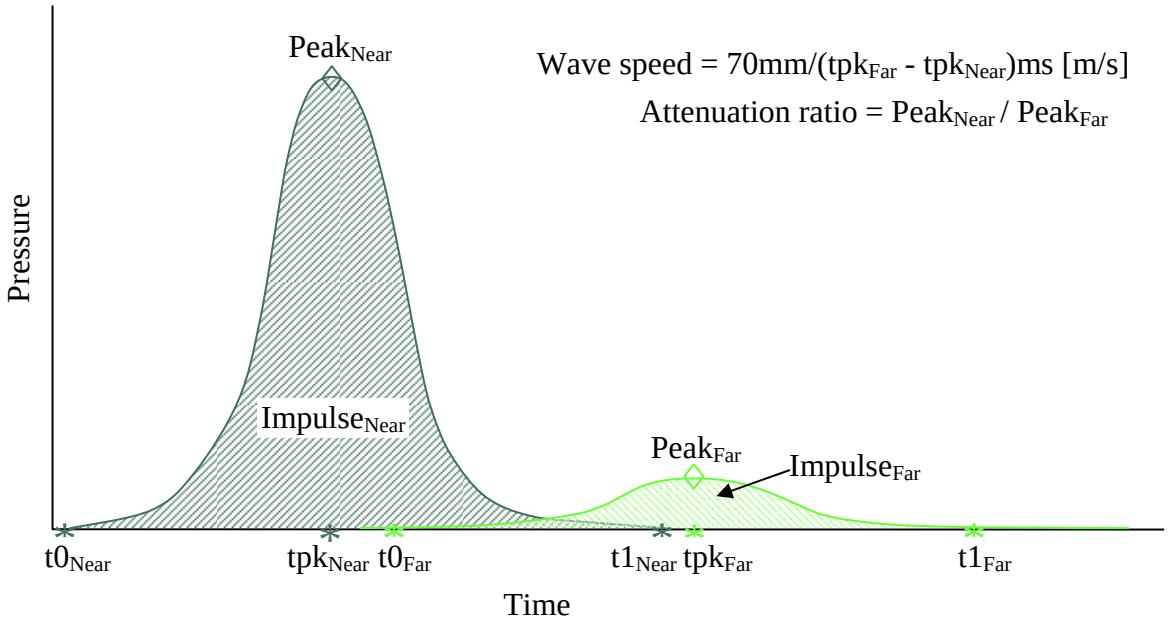

Figure A-4: Graphic of typical pressure profiles for a “near” and “far” transducer on the same side of the injury site, notations indicate the location of points selected for parameter calculation, and derivation of the wave speed and attenuation factor.

APPENDIX B: SUPPLEMENTARY RESULTS

Table 2: Descriptive statistics for the Low Severity injury group.

Parameter	Units	Valid N	Median	Lower Quartile	Upper Quartile	Min.	Max.
Age at Injury	days	6	121.5	115.0	133.0	113.0	138.0
Weight at Injury	kg	6	20.0	20.0	20.0	19.0	22.0
Load (Peak)	N	5	20.8	18.4	21.1	18.2	21.8
Load (Impulse)	N.ms	5	53.9	53.0	57.9	45.1	60.6
Impact Velocity	m/s	3	2.3	2.3	2.3	2.3	2.3
Dural Displacemt.	mm	2	9.2	7.1	11.2	7.1	11.2
Cr-Far, Pre-injury	mmHg	6	5.0	4.4	7.0	1.8	8.1
Ca-Far, Pre-injury	mmHg	6	4.4	2.7	6.8	0.7	7.5
Cr-Far, Peak	mmHg	6	7.2	4.7	7.6	3.8	39.2
Cr-Far, Impulse	mmHg.ms	6	57.7	42.1	266.8	9.6	372.9
Cr-Near, Peak	mmHg	6	565.6	403.0	611.0	96.7	625.6
Cr-Near, Impulse	mmHg.ms	6	1329.5	896.0	1547.5	351.0	1587.2
Ca-Near, Peak	mmHg	6	446.5	370.4	630.5	155.6	680.2
Ca-Near, Impulse	mmHg.ms	6	969.1	869.2	1470.6	539.3	1836.3
Ca-Far, Peak	mmHg	6	21.5	9.2	42.3	1.7	67.6
Ca-Far, Impulse	mmHg.ms	6	209.9	71.2	313.1	12.5	488.1
Cr WaveSpeed	m/s	6	3.4	2.7	9.4	2.5	9.9
Ca WaveSpeed	m/s	6	10.0	7.0	11.0	4.0	12.6
Cr Atten. ratio		6	78.2	20.6	83.0	15.6	106.6
Ca Atten. ratio		6	19.9	16.1	46.4	9.3	93.1

Table 3: Descriptive statistics for the Low Severity injury group.

Parameter	Units	Valid N	Median	Lower Quartile	Upper Quartile	Min.	Max.
Age at Injury	days	6	124.0	121.0	130.0	118.0	135.0
Weight at Injury	kg	6	21.3	19.5	24.0	18.0	26.0
Load (Peak)	N	6	62.1	53.0	65.2	50.2	84.4
Load (Impulse)	N.ms	6	101.5	98.3	101.8	94.9	103.0
Impact Velocity	m/s	5	4.7	4.5	4.8	4.5	4.8
Dural Displacemt.	mm	5	8.3	7.5	10.2	7.3	10.3
Cr-Far, Pre-injury	mmHg	6	7.8	5.5	8.2	4.8	11.1
Ca-Far, Pre-injury	mmHg	6	7.6	6.5	8.9	5.8	8.9
Cr-Far, Peak	mmHg	6	33.7	22.9	80.5	18.5	83.7
Cr-Far, Impulse	mmHg.ms	6	351.2	151.5	432.7	106.1	479.5

Cr-Near, Peak	mmHg	6	1069.0	836.0	1253.0	615.6	1430.3
Cr-Near, Impulse	mmHg.ms	6	1743.7	1553.4	2232.9	1365.7	2504.2
Ca-Near, Peak	mmHg	6	841.7	784.1	989.6	740.3	1015.4
Ca-Near, Impulse	mmHg.ms	6	1572.7	1506.3	1660.1	1046.1	1757.6
Ca-Far, Peak	mmHg	6	46.5	33.3	67.1	23.5	93.0
Ca-Far, Impulse	mmHg.ms	6	402.0	301.1	521.5	188.3	600.4
Cr WaveSpeed	m/s	6	7.2	7.1	11.3	6.7	13.4
Ca WaveSpeed	m/s	6	9.2	8.7	11.0	7.1	15.5
Cr Atten. ratio		6	29.7	17.1	33.2	15.6	41.7
Ca Atten. ratio		6	16.5	13.0	29.7	10.9	34.3

Table 4: Results of the Mann Whitney U-tests comparing the Low and High injury severity groups. Significant results ($p<0.05$) are italicized.

Parameter	**2-sided p value**
Age at Injury	0.589
Weight at Injury	0.485
Load (Peak)	*0.004*
Load (Impulse)	*0.004*
Impact Velocity	*0.036*
Compression	1.000
CSF1MeanPreInj	0.132
CSF4MeanPreInj	*0.041*
CSF1AmplPreInj	0.180
CSF4AmplPreInj	*0.009*
Cr-Far, Peak	*0.026*
Cr-Far, Impulse	*0.041*
Cr-Near, Peak	*0.004*
Cr-Near, Impulse	*0.026*
Ca-Near, Peak	*0.002*
Ca-Near, Impulse	0.093
Ca-Far, Peak	0.132
Ca-Far, Impulse	0.132
Cr Wave speed	0.132
Ca Wave speed	0.937
Cr Atten. ratio	0.180
Ca Atten. ratio	0.589

Table 5: Results of the Wilcoxon Rank Sum (matched-pairs) tests comparing the Cranial and Caudal test parameters. Significant results ($p<0.05$) are italicized.

Parameter	**p-level**
"Far" peak pressure	0.099
"Far" pressure impulse	0.272
"Near" peak pressure	0.136
"Near" pressure impulse	0.071
Wave speed	*0.010*
Attenuation Ratio	0.084